

1  
2  
3  
4  
5  
6  
7  
8  
9  
10  
11  
12  
13  
14  
15  
16  
17  
18  
19  
20  
21  
22  
23  
24  
25  
26  
27  
28  
29

# Measuring Concrete Crosstie Rail Seat Pressure Distribution with Matrix Based Tactile Surface Sensors

*Transportation Research Board 92<sup>nd</sup> Annual Meeting*

Submitted: November 15, 2012



Christopher T. Rapp<sup>1,2</sup>, Marcus S. Dersch<sup>2</sup>, J. Riley Edwards<sup>2</sup>, Christopher P. L. Barkan<sup>2</sup>, Brent Wilson<sup>3</sup>, and Jose Mediavilla<sup>4</sup>

*Rail Transportation and Engineering Center - RailTEC<sup>2</sup>  
Department of Civil and Environmental Engineering  
University of Illinois at Urbana-Champaign  
205 N. Mathews Ave., Urbana, IL 61801*

*Amsted Rail, Inc.<sup>3</sup>  
1700 Walnut St.  
Granite City, IL 62040*

*Amsted RPS<sup>4</sup>  
8400 W. 110<sup>th</sup> St., Ste. 300  
Overland Park, KS 66210*

5827 Words, 2 Tables, 3 Figures = 7077 Total Word Count

Christopher T. Rapp (513) 406-1520 ctrapp3@illinois.edu	Marcus S. Dersch (217) 333-6232 mdersch2@illinois.edu	J. Riley Edwards (217) 244-7417 jedward2@illinois.edu
Christopher P.L. Barkan (217) 244-6338 cbarkan@illinois.edu	Brent Wilson (618) 451-8201 bwilson@amstedrail.com	Jose Mediavilla (913) 345-4807 jose@amstedrps.com

<sup>1</sup> Corresponding author

30 **ABSTRACT**

31 A sustained increase in gross rail loads and cumulative freight tonnages, as well as growing interest in  
32 high speed passenger rail development, is placing an increasing demand on North American railway  
33 infrastructure. To meet this demand, improvements to the performance and durability of concrete  
34 crossties and fastening systems are necessary. One of the typical failure modes for concrete crossties in  
35 North America is Rail Seat Deterioration (RSD), and researchers have hypothesized that localized  
36 crushing of the concrete in the rail seat is one of the potential mechanisms that contributes to RSD. To  
37 better understand this mechanism, the University of Illinois at Urbana-Champaign (UIUC) is using a  
38 matrix based tactile surface sensor (MBTSS) to measure and quantify the forces and pressure distribution  
39 acting at the contact interface between the concrete rail seat and the bottom of the rail pad. Preliminary  
40 data collected during laboratory experimentation has shown that a direct relationship exists between rail  
41 pad modulus and maximum rail seat pressure. Additionally, under a constant vertical load, a direct  
42 relationship between the lateral/vertical (L/V) force ratio and the maximum field side rail seat pressure  
43 has been observed. Given that all preliminary results indicate that various combinations of pad modulus,  
44 track geometry, and L/V force ratios create localized areas of high pressure, crushing remains a potential  
45 mechanism leading to RSD, as will be discussed in this paper. Through the analysis of rail seat pressure  
46 data, valuable insight will be gained that can be applied to the development of concrete crosstie and  
47 fastening system component designs that meet current and projected service demands.

48

## 49 INTRODUCTION

50 Concrete crossties are typically used in locations that place high loading demands on the railroad track  
51 structure and/or necessitate stringent geometric tolerances. In North America, they were adopted in  
52 response to the inability of timber crossties to perform satisfactorily in certain severe service conditions,  
53 such as areas of high curvature, heavy axle load freight traffic, high speed passenger train traffic, high  
54 annual gross tonnages, steep grades, and severe climatic conditions including areas of high moisture that  
55 would cause accelerated decay of timber ties (1). The cast-in shoulders and molded rail seat of concrete  
56 crossties increase their ability to hold gage under these loading conditions (1).

57 Concrete crossties are not without their design and performance challenges. As reported in  
58 surveys conducted by the University of Illinois at Urbana-Champaign (UIUC) in 2008 and 2012, North  
59 American Class I Railroads and other railway infrastructure experts ranked rail seat deterioration (RSD)  
60 as one of the most critical problems associated with concrete crosstie and fastening system performance  
61 (2, 3). Problems that arise from the deterioration of the concrete rail seat surface include widening of  
62 gauge, reduction in the clamping force (toe load) of fastening clips, and insufficient rail cant (2). All of  
63 these problems have the potential to create unsafe operating conditions and an increased risk of rail  
64 rollover derailments (4).

65 A suspected cause of RSD is high forces acting on the concrete rail seat surface, often in  
66 concentrated areas. To address this, a study was performed by the John A. Volpe National Transportation  
67 Systems Center on the effect of wheel/rail loads on concrete tie stresses and rail rollover. The study  
68 confirmed the possibility of concentrated loads producing stresses exceeding the 7,000 psi (48,260 kPa)  
69 minimum design compressive strength of concrete as recommended by the American Railway  
70 Engineering and Maintenance-of-Way Association (AREMA) (4).

71 The combination of static wheel loads and dynamic impact loads impart forces into the rail seat  
72 that potentially damage the concrete surface (5). The magnitude of these loads can vary based on track  
73 support variations, wheel defects, or rail irregularities (5). Well-maintained concrete crosstie track is  
74 typically stiffer than timber crosstie track. According to the AREMA Manual for Railway Engineering,  
75 the typical track modulus value for mainline concrete crosstie track is 6,000 lb/in<sup>2</sup> (41.4 N/mm<sup>2</sup>), which is  
76 approximately twice the typical timber crosstie track modulus of 3,000 lb/in<sup>2</sup> (20.7 N/mm<sup>2</sup>) (6). A track  
77 superstructure that is stiffer, consisting of the rail, fastening system components, and crossties, produces a  
78 less resilient response to impact loads, resulting in higher forces being transferred to the concrete rail seat  
79 surface. This assumes that the track substructures, consisting of the sub-ballast and ballast layers, for  
80 both concrete and timber crosstie track, provide adequate support conditions for each track type. Despite  
81 being a less resilient track superstructure, a study performed to investigate the effect of replacing  
82 defective timber crossties with concrete crossties yielded results showing a drastic improvement on the  
83 remaining life of other crossties for this given section of track (7).

84 To better understand the forces acting at this surface, researchers at UIUC are using matrix based  
85 tactile surface sensors (MBTSS) as a means to measure load magnitude and distribution. MBTSS have  
86 been previously used in experimentation under the tie plates on timber crossties (8); however, researchers  
87 at UIUC are using this technology to explore the pressure distribution on the rail seats of concrete  
88 crossties.

## 90 Background

91 There are many factors that affect the rail seat pressure distribution, one of which is the transfer of forces  
92 at the wheel/rail interface. The transfer of forces from the wheel to the rail is heavily dependent upon  
93 frictional characteristics at this interface, such as the presence of top-of-rail (TOR) friction modifiers (9).  
94 After the load is transferred from the wheel to the rail, it moves through the web of the rail and into the  
95 base of the rail. Next, the load is distributed through the rail pad assembly onto the rail seat of the  
96 crosstie. The profile of the wheel and rail (e.g. wear pattern), and the performance of the rail car truck,  
97 are some of the variables that can govern the location and angle of the resultant force. The authors of this  
98 paper suspect that these parameters can cause significant variation in which areas of the rail seat are  
99 receiving concentrated loadings. Additionally, the lateral to vertical (L/V) ratio of this resultant force also

100 varies greatly depending on track geometry conditions. Lateral forces imparted onto the rail can be  
 101 significant in horizontal curves or special trackwork. Trains travelling at speeds above or below the  
 102 balancing speed of a curve can cause shifts in the vertical and lateral load to the high or low rail,  
 103 respectively. These loads being imparted into the track structure are highly dependent on the speed  
 104 through which a train is operating through the curve, and it is understood that trains do not always travel  
 105 at the design balance speed (10). These loading scenarios are especially likely on shared infrastructure,  
 106 where both freight and passenger trains operate on the same track, typically at different speeds, which can  
 107 vary as much as 100 mph (161 kph). Passenger trains operating at higher speeds on a track designed  
 108 primarily for freight traffic would be operating at a cant deficiency, where axle loads are not evenly  
 109 distributed between even rails, and forces on the high rail and fastening system components are higher.  
 110 As a result, shared infrastructure presents diverging engineering requirements for track that can  
 111 accommodate the heavy axle loads of slower speed freight trains with the possibility of high dynamic  
 112 loads from higher speed passenger trains.

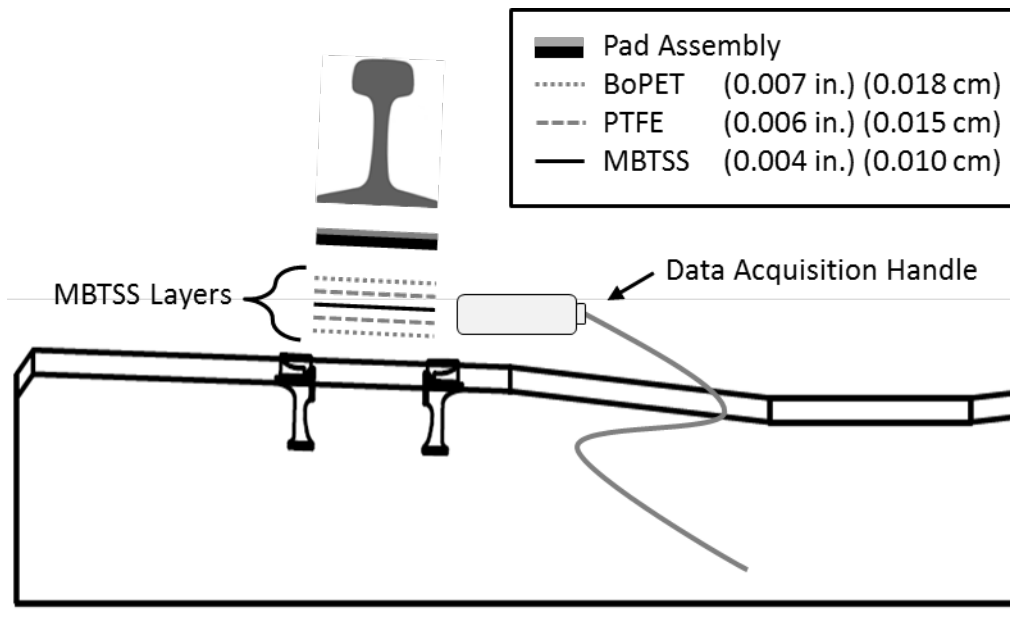
113 Design of the fastening system components also plays a crucial role in the distribution of pressure  
 114 in the rail seat. Given the stiff nature of concrete cross-tie track, the fastening system must provide some  
 115 of the resiliency necessary to attenuate loads without damaging the concrete (11). Some of the variables  
 116 potentially affecting the magnitude and distribution of pressure on the concrete rail seat are explored  
 117 through laboratory experimentation. Preliminary results from these experiments are documented in this  
 118 paper.

119

### 120 Sensor Technology and Protection

121 The sensor technology UIUC is currently using for quantifying forces and pressure distribution at the rail  
 122 seat is the MBTSS manufactured by Tekscan® Inc. In order to protect the MBTSS from shear forces and  
 123 puncture, it is covered on both sides with thin layers of polytetrafluoroethylene (PTFE) and bi-axially  
 124 oriented Polyethylene Terephthalate (BoPET) (Figure 1). Calibration of MBTSS is conducted by  
 125 applying known loads and correlating the loads with the respective raw sum units. Known input loads  
 126 can also be applied to collected MBTSS data in order to quantify pressure distributions.

127



128

129

130

131

132

FIGURE 1 Profile View of MBTSS Layers and Thicknesses.

### 133 **Experimental Setup**

134 UIUC's experimental testing was performed at the Advanced Transportation Research and Engineering  
135 Laboratory (ATREL). The Pulsating Load Testing Machine (PLTM), which is owned by Amsted RPS  
136 and was designed to perform the American Railway Engineering and Maintenance-of-way Association  
137 (AREMA) Test 6 (Wear and Abrasion), as well as other experiments related to concrete crossties and  
138 fastening systems, was used to execute the experiments within this paper. The PLTM consists of one  
139 horizontal and two vertical actuators, both attached to a steel loading head that encapsulates a 24 inch  
140 (610 mm) section of rail. The rail section is attached to one of the two rail seats on a concrete crosstie.  
141 Preliminary UIUC research included installing a MBTSS in the concrete crosstie fastening system and  
142 loading the tie using the PLTM. Loading inputs for this experimentation are applied to the rail in only the  
143 vertical and lateral directions, due to the constraints of the experimental setup. UIUC researchers  
144 recognize that moving wheel loads impart longitudinal forces onto the track structure that add a higher  
145 level of complexity to analysis of loads on the various track components. Although it is possible that the  
146 longitudinal forces would have a large effect on varying the pressure distribution at the rail seat, the  
147 ability to simulate such loads with this experimental setup does not currently exist.

148

### 149 **RESULTS OF EXPERIMENTATION**

150 Experiments have been conducted by UIUC researchers to collect data on the distribution of pressure on  
151 the concrete crosstie rail seat based on expected loading conditions at the rail seat surface. The  
152 experimental setup is not meant to replicate the common field loading conditions, but is designed to  
153 simulate extreme loading conditions that can occur in the field. Therefore, this experimental setup  
154 simulates a single wheel load imparted onto a single crosstie.

155 These experiments were conducted to analyze and quantify the loading behavior at this interface  
156 using a variety of load inputs while varying concrete crosstie fastening system components. The first  
157 series of experiments was performed to determine a relationship between the rail pad modulus and  
158 pressure distribution at the rail seat. The modulus of a rail pad is often considered to be a proxy for the  
159 stiffness of the pad. However, it should be noted that modulus is a property of the material, while  
160 stiffness is dependent on both the material properties and the boundary conditions of the component.  
161 Another series of experiments was performed to compare two different elastic fastening system clip  
162 designs with respect to their ability to distribute pressure over the rail seat. For each series of  
163 experiments, various L/V force ratios were explored in an attempt to simulate a variety of rail vehicle and  
164 track interaction conditions that could occur at the wheel/rail interface. The overall objective of this  
165 experimentation was to determine a relationship between L/V force ratio and pressure distribution at the  
166 rail seat while varying different components of the fastening system. The following sections explain the  
167 effect of varying L/V force ratios, and present the experimental protocol and results from the  
168 aforementioned experiments. There are many variables that can affect the L/V force ratio, including the  
169 track geometry (e.g. horizontal curvature), wheel/rail interface conditions and frictional properties, axle  
170 loads, railcar truck steering performance, and train speed (12). Researchers at UIUC suspect that a high  
171 concentration of field side loading could be seen on the high rail seat on a section of superelevated track  
172 with a train operating in an underbalanced condition, and that, inversely, a field side concentration on the  
173 low rail seat would be expected for a train operating in an overbalanced condition.

174

### 175 **Rail Pad Component Experimentation**

176 Concrete crosstie fastening systems typically include a single or multi-layer rail pad assembly (13). Part  
177 of this assembly includes a polymer rail pad, historically made of rubber or polyethylene, to attenuate the  
178 load and provide protection for the concrete rail seat (1). Given that concrete crosstie track is often more  
179 rigid than the traditional timber crosstie track, concrete crossties can impart higher stresses onto the  
180 ballast. An important purpose of the rail pad as an individual component is to provide increased  
181 resiliency for the concrete crosstie system. The increased resiliency provides the advantages of  
182 dampening the loads experienced by the rolling stock and increasing passenger comfort (14). Rail pads

183 are manufactured from a variety of materials and molded into different geometries. Their material  
184 properties and component geometries govern the modulus and stiffness values for a given design.

185 Part of the research being conducted at UIUC is investigating the effect of the rail pad's modulus  
186 on mitigating high loads imparted on the rail seat while continuing to protect the concrete rail seat.  
187 Researchers at UIUC are exploring the possibility that a rail pad of a lower modulus (i.e. softer) will  
188 distribute the applied load over a wider area of the concrete rail seat. Although a softer rail pad may  
189 better mitigate high impact loads, its high resiliency allows for greater rail deflection, which can increase  
190 wear and fatigue of other components of the fastening system (1). The softer pad, in combination with  
191 the elastic clips commonly used in concrete crosstie fastening systems, can perform well in moderate  
192 traffic loading conditions (13). Under heavier loads, as are becoming increasingly common in North  
193 America, excessive lateral movement of the rail base and wear of the fastening system components can  
194 occur (13).

195 In performing the AREMA Test 6 (Wear and Abrasion) using the PLTM, researchers at UIUC  
196 have seen this excessive lateral movement of the rail cause wear on the field side cast-in steel shoulder,  
197 which could potentially lead to gauge-widening. In both the 2008 and 2012 surveys of North American  
198 Class I Railroads, shoulder/fastener wear or fatigue ranked second behind RSD as the second most critical  
199 concrete tie problem (2, 3). Also, UIUC researchers are exploring the possibility that a rail pad with  
200 higher modulus will help reduce the stress on the fastening system as a whole, but will place a higher  
201 concentration of load on the concrete rail seat surface, and in turn result in increased ballast pressures on  
202 the bottom of the crosstie (13).

203 An experiment was performed to compare the pressure distributions of a higher modulus, medium  
204 density polyethylene (MDPE) rail pad, a lower modulus Thermoplastic Vulcanizate (TPV) rail pad, and a  
205 more commonly used two-part pad assembly comprising of a Nylon 6-6 abrasion plate and a 95 Shore A  
206 Thermoplastic Polyurethane (TPU) pad. The MDPE and TPV rail pads used were cast with a flat surface  
207 specifically for this experiment to remove variation in pad geometry. The MDPE pad had a Shore  
208 Hardness of 60 on the D scale, with a flexural modulus of 120,000 psi (827.4 N/mm<sup>2</sup>). The TPV pad had  
209 a Shore Hardness of 86 on the A scale, with an approximate flexural modulus of 15,000 psi (103.4  
210 N/mm<sup>2</sup>) (this value is based on a TPV with a similar Shore Hardness of 87A). Although the numerical  
211 value for the TPV rail pad Shore Hardness is higher than that of the MDPE, the type A scale is used for  
212 softer plastic materials, whereas the type D is used for harder plastic materials. In this instance, the value  
213 of 60 for the type D scale indicates a harder material than the values of 86 and 95 for the type A scale.

214 Loading conditions were consistent for the three series of experiments, having a constant vertical  
215 load of 32,500 lb (144.6 kN) and corresponding lateral loads based on the L/V force ratios being  
216 simulated. This magnitude of vertical load was chosen because it is the same value as specified for the  
217 AREMA Test 6 (Wear and Abrasion), which is designed to simulate a heavy-axle freight car negotiating a  
218 sharp curve. To compare the relative performances of the three rail pad components, the maximum  
219 loaded frame per L/V force ratio was identified and obtained for each pad (Table 1a). Table 1b is a  
220 compilation of the results from this series of experiments. The data collected for each rail pad component  
221 is presented side-by-side per L/V force ratio to show the difference in pressure distribution for the various  
222 materials under identical loading conditions. Figures 2a, 2b, and 2c are plots of the average pressure per  
223 column of data from the MBTSS along the width of the sensor on the rail seat for the TPV, MDPE, and  
224 two-part pad assemblies, per L/V force ratio.

225

226

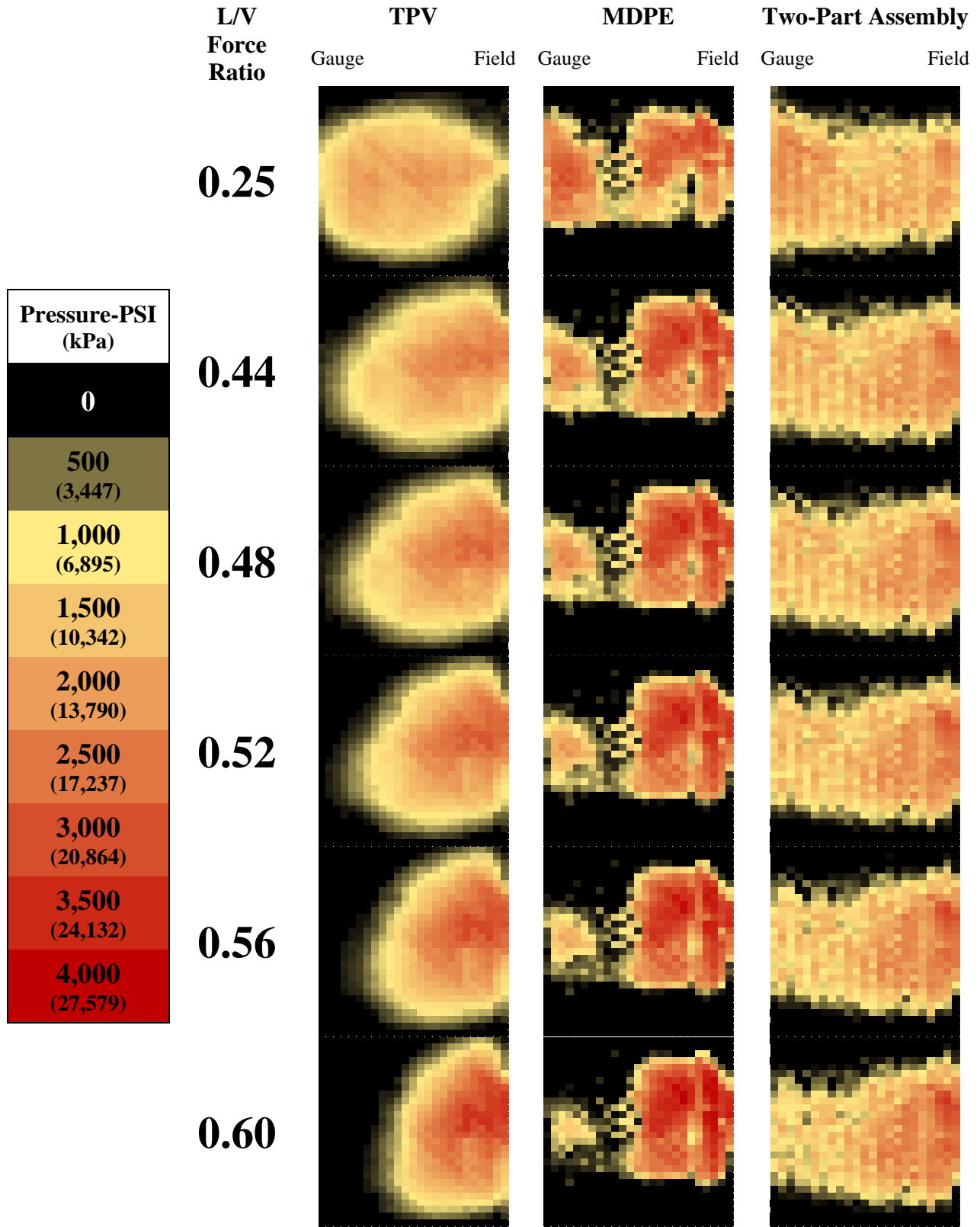


TABLE 1a Rail Seat Pressure Distributions for Rail Pad Assemblies under Varying L/V Force Ratios.

227  
228  
229

230  
231**TABLE 1b Results of Rail Pad Component Experimentation**

<b>L/V Force Ratio</b>	<b>0.25</b>			<b>0.44</b>		
<b>Pad Assembly</b>	<b>MDPE</b>	<b>TPV</b>	<b>2-Part Pad</b>	<b>MDPE</b>	<b>TPV</b>	<b>2-Part Pad</b>
<b>Vertical, kips</b>	32.50	32.50	32.50	32.50	32.50	32.50
<b>Lateral, kips</b>	8.13	8.13	8.13	14.30	14.30	14.30
<b>Contact Area, in<sup>2</sup></b>	20.09	28.75	24.73	19.31	27.93	23.96
<b>Peak Pressure, psi</b>	3,213	2,139	2,460	3,469	2,573	2,821
<b>Contact Area over 3000 psi, in<sup>2</sup></b>	0.34	0	0	1.55	0	0

<b>L/V Force Ratio</b>	<b>0.48</b>			<b>0.52</b>		
<b>Pad Assembly</b>	<b>MDPE</b>	<b>TPV</b>	<b>2-Part Pad</b>	<b>MDPE</b>	<b>TPV</b>	<b>2-Part Pad</b>
<b>Vertical, kips</b>	32.50	32.50	32.50	32.50	32.50	32.50
<b>Lateral, kips</b>	15.60	15.60	15.60	16.90	16.90	16.90
<b>Contact Area, in<sup>2</sup></b>	19.12	27.25	23.91	19.02	25.75	23.86
<b>Peak Pressure, psi</b>	3,546	2,800	2,877	3,721	2,925	2,990
<b>Contact Area over 3000 psi, in<sup>2</sup></b>	2.32	0	0	2.86	0	0

<b>L/V Force Ratio</b>	<b>0.56</b>			<b>0.60</b>		
<b>Pad Assembly</b>	<b>MDPE</b>	<b>TPV</b>	<b>2-Part Pad</b>	<b>MDPE</b>	<b>TPV</b>	<b>2-Part Pad</b>
<b>Vertical, kips</b>	32.50	32.50	32.50	32.50	32.50	32.50
<b>Lateral, kips</b>	18.20	18.20	18.20	19.50	19.50	19.50
<b>Contact Area, in<sup>2</sup></b>	18.63	23.96	23.38	17.76	21.30	23.38
<b>Peak Pressure, psi</b>	3,838	3,162	3,201	4,096	3,400	3,325
<b>Contact Area over 3000 psi, in<sup>2</sup></b>	3.44	0.53	0.10	4.11	1.74	0.29

232

233

234  
235

*NOTE: 1 kip = 4.45 kN, 1 in<sup>2</sup> = 6.45 cm<sup>2</sup>, 1 psi = 6.89 kPa*



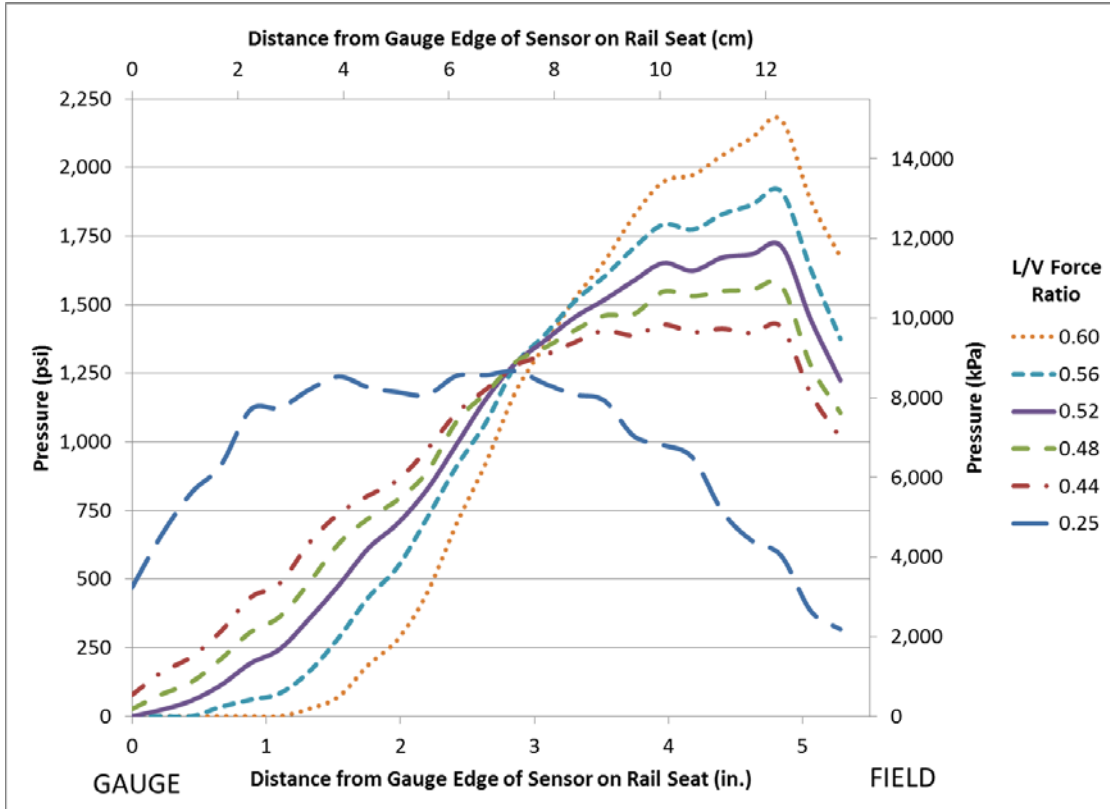


FIGURE 2a Average Pressure Distributions for TPV Rail Pad.

236  
237  
238

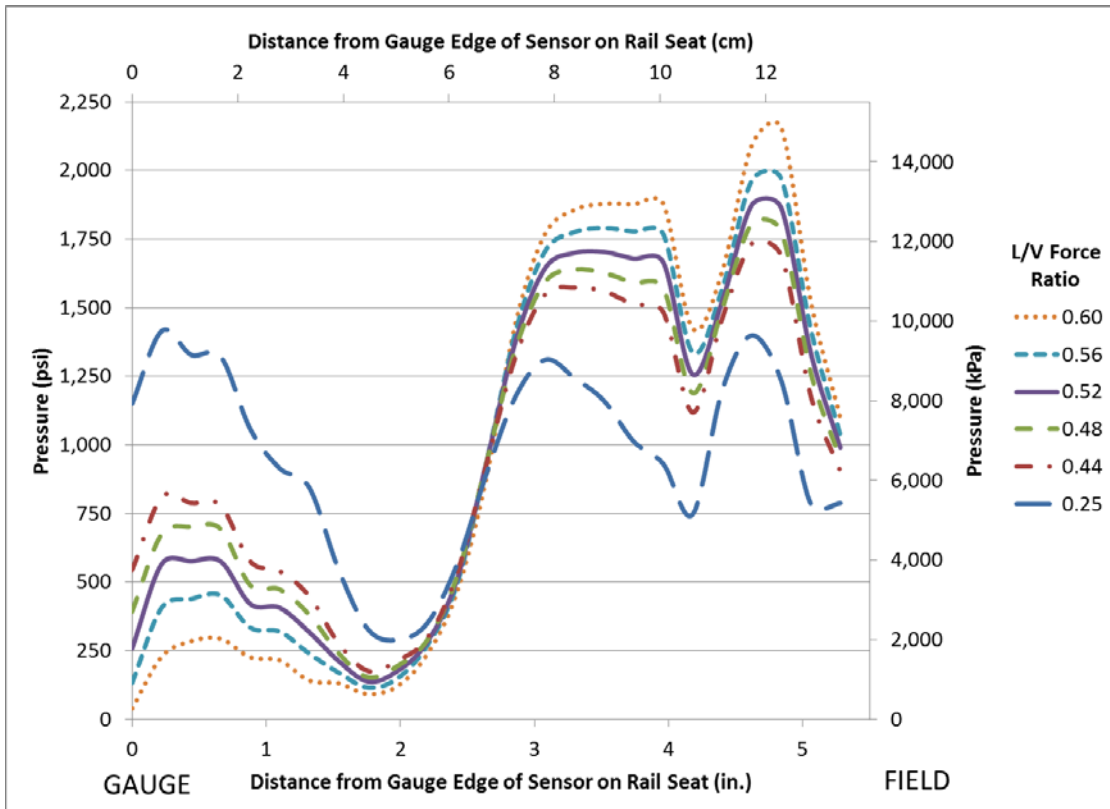
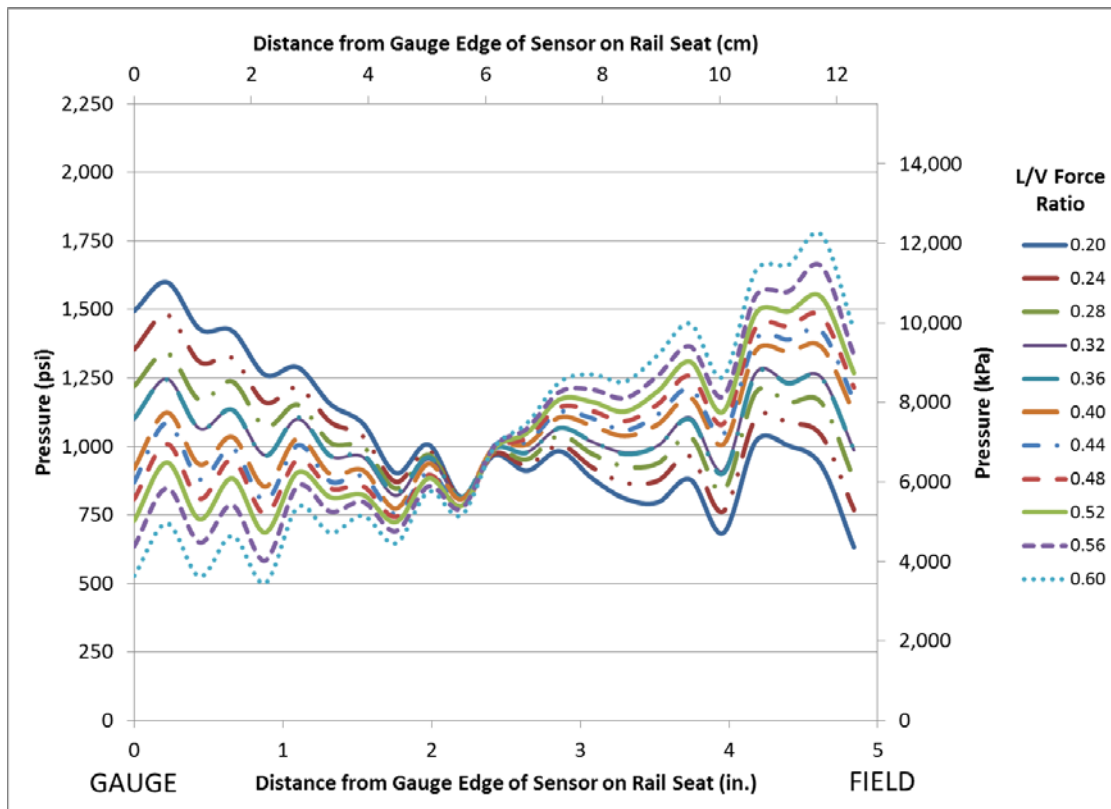


FIGURE 2b Average Pressure Distributions for MDPE Rail Pad.

239  
240

241



**FIGURE 2c Average Pressure Distributions for Two-Part Pad Assembly.**

242  
243  
244

245 This experiment shows that the MDPE rail pad distributed the same applied load over a  
246 noticeably smaller area of the rail seat than the low modulus TPV rail pad or two-part pad assembly. For  
247 an L/V force ratio of 0.25, the contact area of the load for the high modulus MDPE rail pad was 20.09 in<sup>2</sup>  
248 (129.61 cm<sup>2</sup>), only 70% the amount of 28.75 in<sup>2</sup> (185.48 cm<sup>2</sup>) of contact area recorded for the low  
249 modulus TPV rail pad under the same load, and only 81% the amount of 24.73 in<sup>2</sup> (159.55 cm<sup>2</sup>) of the  
250 contact area for the two-part pad assembly. Peak pressures for each of the three pad assemblies occurred  
251 during the L/V force ratio of 0.60, as it was the same vertical load being applied to smaller contact areas.  
252 Of the three pad assemblies used in experimentation, the highest peak pressure recorded was for the  
253 MDPE rail pad, with a value of 4,096 psi (28,240 kPa). This value is approximately 20% higher than the  
254 peak pressure of 3,400 psi (23,440 kPa) recorded for the TPV rail pad, and 23% higher than the 3,325 psi  
255 (22,930 kPa) recorded for the two-part pad assembly. The MDPE pad distributed this same load over  
256 11% less of the rail seat surface than the TPV rail pad, and 17% less than the two-part pad assembly, thus  
257 resulting in the higher peak pressures. Furthermore, although the MDPE rail pad had a smaller total  
258 contact area, it had a larger amount of area loaded at higher pressures than the two other pad components  
259 used in experimentation, as is evident in the rows showing contact area over 3,000 psi (20,680 kPa)  
260 (Table 1b).

261 In Figures 2a, 2b, and 2c, the increase of loading into the field side of the rail seat as L/V force  
262 ratio increases can be seen for all three rail pad assemblies used in experimentation. In Figure 2c, a wider  
263 range of more uniformly incremented L/V force ratios are presented to better show the transfer of the  
264 pressure distributed towards the field side of the rail seat. In all three instances, the decrease of pressure  
265 in the area immediately adjacent to the field side shoulder is likely due to the gap beneath the insulator  
266 post beyond the width of the base of the rail. The shape of the curves for each experiment could be due to  
267 variable material geometry or properties, which can in turn govern the rail base rotation, of each rail pad  
268 material under increasing L/V force ratios. Additional experimental replicates are needed to gain further

269 insight on the shape of the curve on an average rail seat. The curves for the TPV pad are similar to the  
270 theoretical triangular distribution pattern noted in previous concrete crosstie rail seat stress research (4).  
271 This could be due to the fact that the lower modulus of the TPV pad allows the base of the rail to rotate  
272 more under increased lateral loads. The higher modulus MDPE pad, however, would allow less rotation  
273 of the rail base, resulting in the distributions shown in Figure 2b. Supporting the possibility that a rail pad  
274 component with a lower modulus could allow greater rotation of the base of the rail is the fact that the  
275 largest decrease in contact area under increasing L/V force ratio occurred for the TPV rail pad. A  
276 decrease of approximately 26% of contact area occurred between the L/V force ratios of 0.25 and 0.60 for  
277 the TPV rail pad, as compared to 12% and 5% for the MDPE pad and two-part assembly, respectively.

278 The behavior of the commonly used two-part pad assembly can be seen as a hybrid of the higher  
279 modulus MDPE pad and the lower modulus TPV pad. The peak pressure values were on average closer  
280 to those of the TPV pad, while undergoing the least change in contact area under increasing L/V force  
281 ratio of the three pad components used in experimentation. However, the ability of the two-part pad  
282 assembly to resist rotation of the rail base more closely mirrored that of the MDPE pad, as the decrease in  
283 contact area under increasing L/V force ratios between these two components was more similar to that of  
284 the TPV rail pad. This similarity can also be seen in Table 1a, where under an L/V force ratio of 0.60,  
285 both the MDPE and two-part pad assemblies retained contact on the gauge side of the rail seat, whereas  
286 this area under the TPV rail pad became unloaded.

287 For this experiment, and the following clip component experiment, data was not collected in the  
288 area immediately adjacent to the gauge side of the rail seat. Figures 2a, 2b, and 2c, show that the width of  
289 the sensor on the x-axis is less than the actual full width of the rail seat used for experimentation. This is  
290 due to the need to protect the MBTSS by allowing the conductive leads extending from the pressure  
291 sensitive area of the sensor to lay flat on the rail seat, rather than bending that area over the base of the  
292 rail. Bending of the sensor around the base of the rail was found to cause damage to the sensor in earlier  
293 experimentation. Sacrificing data on the gauge side was accepted by the researchers at UIUC, as the  
294 pressures near the field side were the primary target of this investigation.

295 From this experiment, it can be seen that a direct relationship exists between a high rail pad  
296 modulus and concentrated loading of the rail seat. Furthermore, a highly concentrated loading of the rail  
297 seat could lead to crushing of the concrete surface; although the peak pressure values recorded in this  
298 laboratory experimentation did not approach the AREMA recommended minimum 28-day-design  
299 compressive strength of concrete used for concrete ties of 7,000 psi (48,260 kPa) (6). It is also possible  
300 that highly concentrated loads could be seen in the field because although the maximum vertical load  
301 explored in this laboratory experimentation was only 32.5 kips (144.56 kN), wheel impact load detector  
302 (WILD) sites in revenue service can record loads of greater than 100 kips (444.82 kN) (15). It is likely  
303 that a load of this magnitude would produce pressures on the rail seat in excess of 7,000 psi (48,260 kPa).

304 Another parameter that could affect the rail pad's ability to evenly distribute pressure is dynamic  
305 load attenuation. Under repeated loading cycles, such as those imparted by unit coal trains, the inability  
306 for the pad to fully recover elastically between axles could lead to changes in the distribution of pressure  
307 on concrete rail seats. Investigation into repeated loadings of rail pads could also lead to discussion of the  
308 effect of wear life of this component on rail seat pressure distribution

309

### 310 **Fastening Clip Experimentation**

311 Fastening systems for concrete crossties serve the primary purposes of providing vertical, lateral, and  
312 longitudinal restraint of the rail and providing load attenuation. A variety of clip designs and rail pad  
313 materials result in concrete crosstie and elastic fastening systems with unique stiffness characteristics,  
314 which result in a variety of specialized performance capabilities (13). An experiment was performed to  
315 investigate pressure distribution on the rail seat while varying the clip component of a concrete crosstie  
316 fastening system. Two common North American fastening system clip designs were used for this  
317 experiment, which will be referred to as Clip A and Clip B (Table 2a). The design clamping force for  
318 Clip A was 4,750 lbs (21.1 kN), with a spring rate of 8,223 lb/in (14.4 kN/cm). The design clamping force

319 for Clip B was 5,500 lbs (24.5 kN), with a spring rate of 6,286 lb/in (11.0 kN/cm). The spring rate values  
320 were determined based on the manufacturer's design clamping force at a given deflection.

321 The same two-part rail pad assembly was used for each clip to hold that variable constant. It  
322 should be noted that a different concrete cross-tie was used for each respective clip experiment, as the cast-  
323 in steel shoulder design for each fastening system was different (a requirement of different fastening  
324 systems). This could result in variability in pressure distributions due to minor differences in the concrete  
325 rail seat profile; however, these differences should not be significant.

326 Loading conditions were consistent for this experiment, having a constant vertical load of 32,500  
327 lb (144.6 kN) and corresponding lateral loads based on the L/V force ratios simulated. Four L/V force  
328 ratios were used for this experiment, ranging from 0.25 to 0.60. To compare the relative performances of  
329 the two clip designs, the maximum loaded frame per L/V force ratio was obtained for each clip (Table  
330 2a). Table 2b is a summary of results from these maximum loaded frames. Figure 3a is a plot of the  
331 average pressure per column of data from the MBTSS along the width of the sensor on the rail seat for  
332 Clip A, per L/V force ratio. Figure 3b is the same plot of data collected during the experiment for Clip B.  
333

334

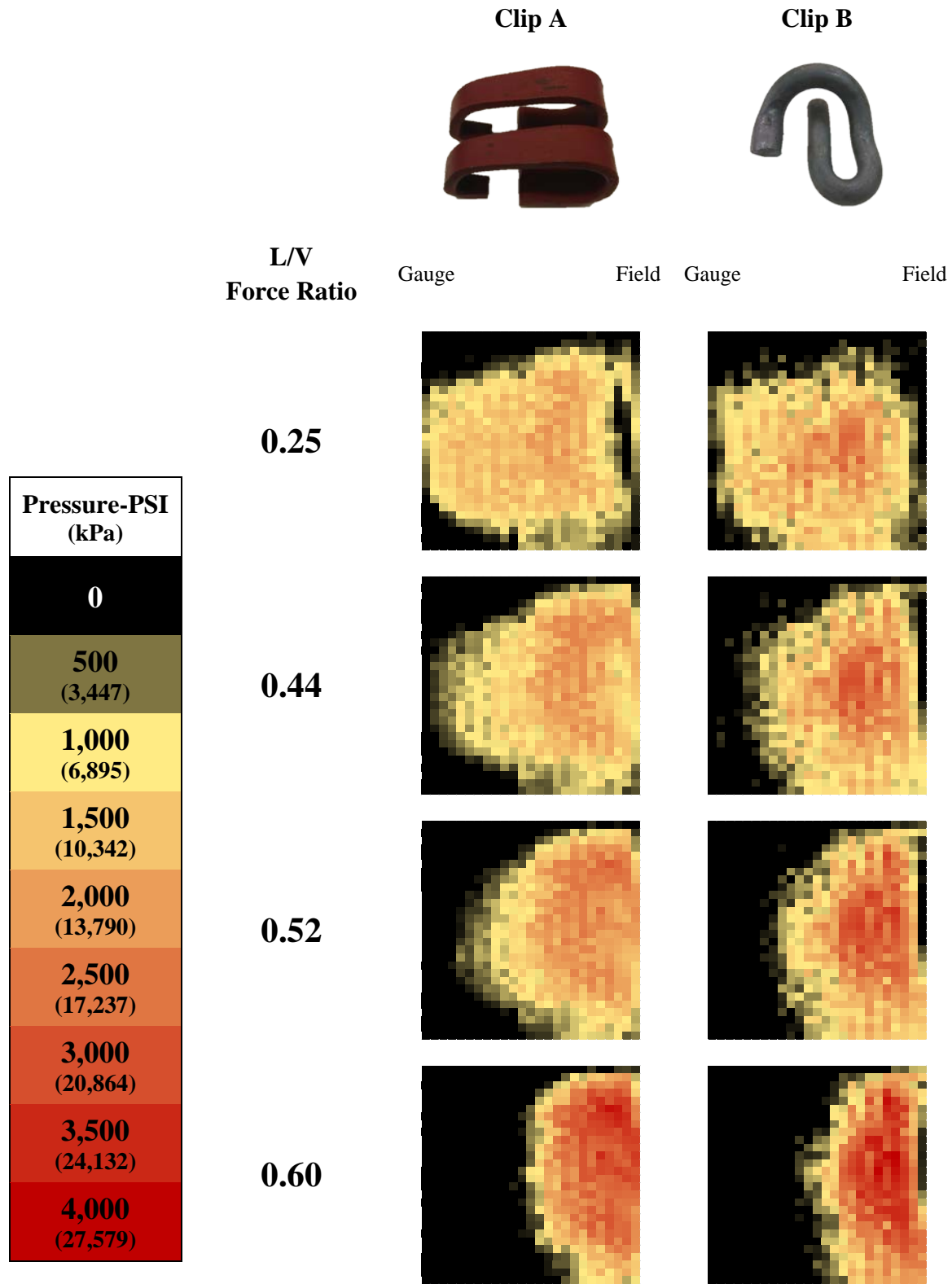


Table 2a Comparison of Rail Seat Pressure Distributions for Two Differing Fastening Clips.

335  
336  
337**TABLE 2b Results of Fastening Clip Experiment**

<b>L/V Force Ratio</b>	<b>0.25</b>		<b>0.44</b>	
<b>Clip Design</b>	<b>Clip A</b>	<b>Clip B</b>	<b>Clip A</b>	<b>Clip B</b>
<b>Vertical, kips</b>	32.50	32.50	32.50	32.50
<b>Lateral, kips</b>	8.13	8.13	14.30	14.30
<b>Contact Area, in<sup>2</sup></b>	28.36	27.59	26.57	24.54
<b>Peak Pressure, psi</b>	2,188	2,744	2,327	3,067
<b>Contact Area over 3000 psi, in<sup>2</sup></b>	0	0	0	0.24

<b>L/V Force Ratio</b>	<b>0.52</b>		<b>0.60</b>	
<b>Clip Design</b>	<b>Clip A</b>	<b>Clip B</b>	<b>Clip A</b>	<b>Clip B</b>
<b>Vertical, kips</b>	32.50	32.50	32.50	32.50
<b>Lateral, kips</b>	16.90	16.90	19.50	19.50
<b>Contact Area, in<sup>2</sup></b>	23.62	21.01	16.55	17.18
<b>Peak Pressure, psi</b>	2,872	3,385	3,809	4,083
<b>Contact Area over 3000 psi, in<sup>2</sup></b>	0	0.92	2.13	3.53

338

339  
340

*NOTE: 1 kip = 4.45 kN, 1 in<sup>2</sup> = 6.45 cm<sup>2</sup>, 1 psi = 6.89 kPa*

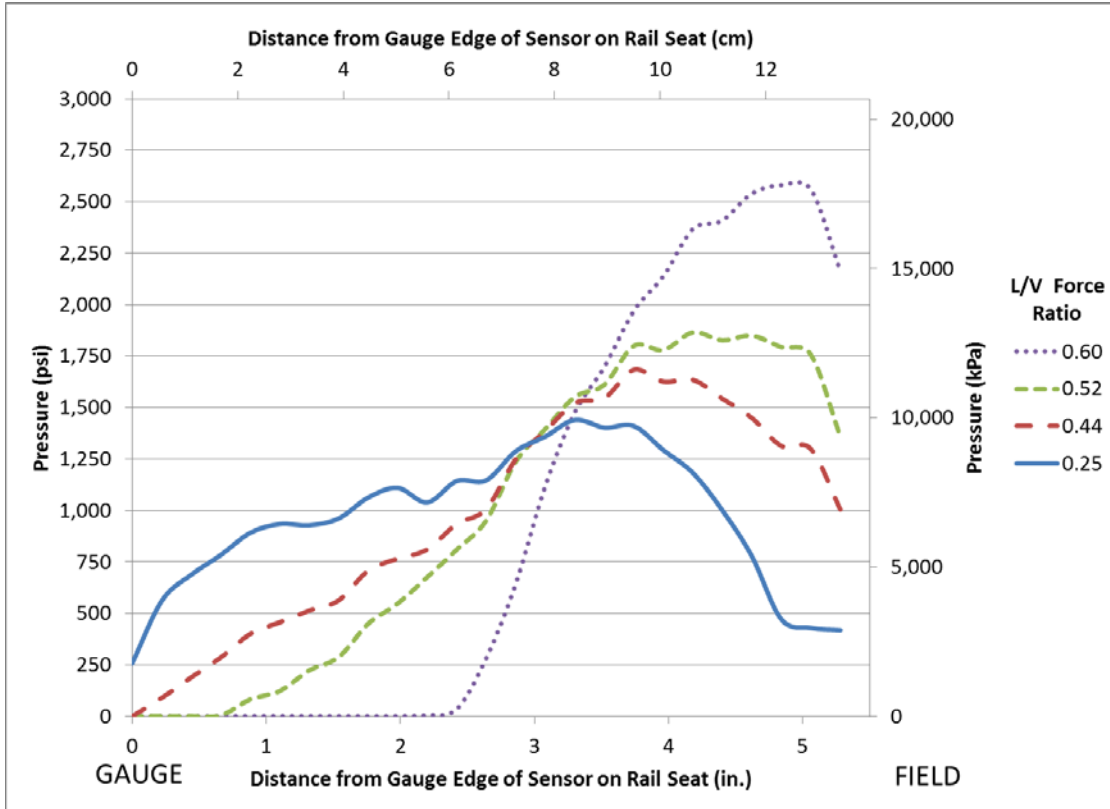


FIGURE 3a Average Pressure Distributions for Clip A.

341  
342  
343

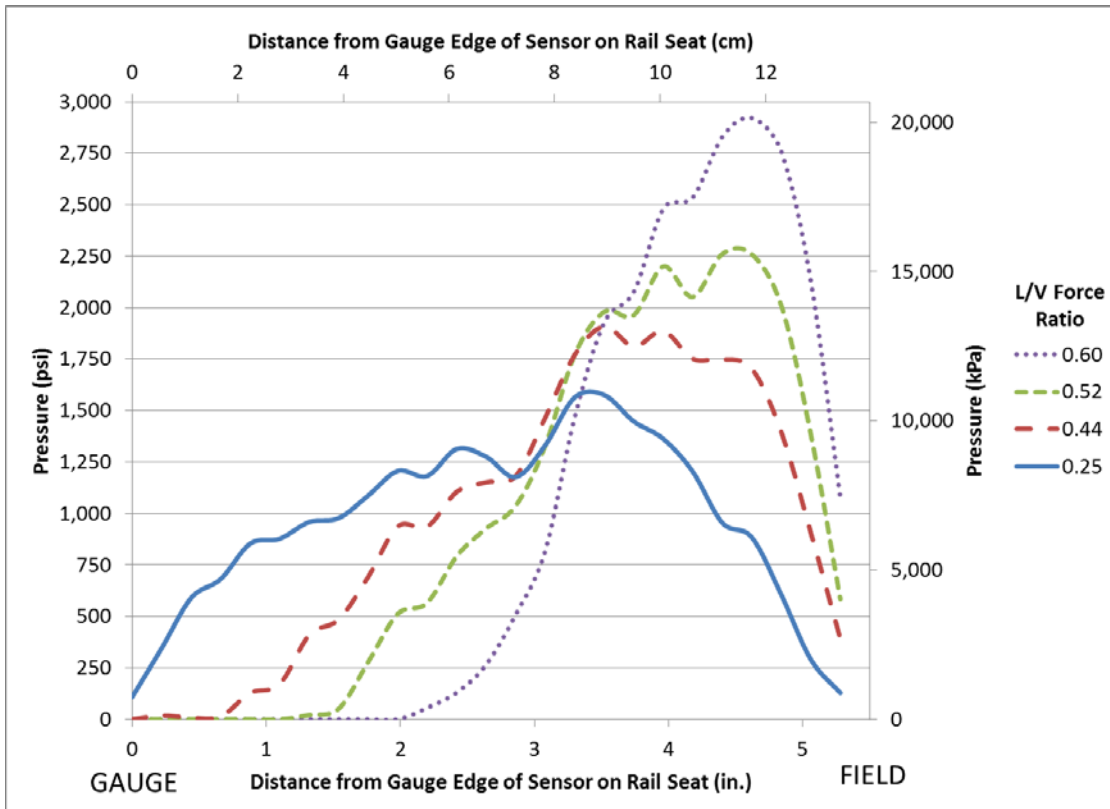


FIGURE 3b Average Pressure Distributions for Clip B.

344  
345

346 Results from this experiment show a lower magnitude of variability between these two fastening  
347 system components than results from earlier experimentation with different rail pad moduli. The general  
348 trend was that Clip A distributed the pressure over a slightly larger area, thus producing lower peak  
349 pressure values. The greatest difference in contact area between the two clips was 2.61 in<sup>2</sup> (16.84 cm<sup>2</sup>), at  
350 an L/V force ratio of 0.52. At the most extreme L/V force ratio of the experiment, the difference in peak  
351 pressures was only 274 psi (1,890 kPa), with the value for Clip B being 7.2% higher than that of Clip A.

352 A notable difference between the results from the two clips is the shape of the pressure  
353 distributions. It appears that the geometry of each clip effects where load is concentrated on the rail seat,  
354 but it should be noted that no replicates using additional crossties or fastening systems have been  
355 conducted. In all of the pressure distribution frames for Clip B, a central area of concentrated pressure is  
356 noted, and the design of this clip is such that there is one point of contact between the clip and in the  
357 insulator resting on the rail base, as can be seen in Table 2a. For Clip A distributions, the peak pressures  
358 appear to be concentrated over a wider area of the rail seat, and not concentrated on a single area like Clip  
359 B. This appears logical, as the design of Clip A has two points of contact between the clip and insulator,  
360 as can be seen in Table 2a. This concept is also supported by the fact that the Clip B experiments showed  
361 higher peak pressures being imparted into the rail seat, while having smaller contact areas than Clip A for  
362 all but the L/V force ratio of 0.60. Whether these same pressure distributions are seen in the field is not  
363 yet known, which researchers at UIUC intend to investigate through future field experimentation.

## 364 **CONCLUSIONS AND FUTURE WORK**

365 The following conclusions can be drawn from the analysis of data collected in these preliminary  
366 experiments using MBTSS:

- 367 • Lower modulus rail pads distribute rail seat loads over a larger contact area, reducing peak  
368 pressure values and mitigating highly concentrated loads at this interface
- 369 • Higher modulus rail pads distribute rail seat loads in more highly concentrated areas, possibly  
370 leading to localized crushing of the concrete surface under extreme loading events
- 371 • A more commonly used two-part pad assembly comprising of both higher and lower modulus  
372 materials can provide the benefits of reducing peak pressure values while maintaining a more  
373 constant contact area under increasing L/V force ratios and reducing rail base rotation
- 374 • A lower L/V force ratio of the resultant wheel load distributes the pressure over a larger contact  
375 area
- 376 • A higher L/V force ratio of the resultant wheel load causes a concentration of pressure on the  
377 field side of the rail seat, resulting in higher peak pressures
- 378 • The design of the clip component of the fastening system affects the shape of the pressure  
379 distribution on the rail seat
- 380 • No large differences in peak pressure or contact area values were seen between the two clip  
381 designs used in experimentation
- 382
- 383

384 Given the projected increase in the use of concrete crossties in the North American railroad  
385 industry, research will continue at UIUC to develop a comprehensive laboratory and field instrumentation  
386 plan to better understand interactions at this interface. The experiments described in this paper were  
387 theoretical in nature, with the loading conditions chosen by researchers based on expert opinion and  
388 working knowledge of rail seat loads.

389 Future laboratory experimentation planned by researchers at UIUC includes installing MBTSS on  
390 rail seats of concrete crossties with various models of fastening systems to further view the effect that  
391 variations in clip design have on rail seat pressure distribution. Additional rail pad component  
392 experimentation will take place to better understand the material properties of this component and the  
393 effect it has on mitigating rail seat pressures. Experiments with rail pads of varying thicknesses will also  
394 be performed to better understand the effect on rail seat pressure distribution, as rail pad thickness was not  
395



396 a variable in the initial pad component experimentation. Since a load applied to a larger contact area  
397 appears to result in lower peak pressure values, experiments will also be conducted on crossties with  
398 various rail seat dimensions and degrees of deterioration and/or repair via epoxy or other materials.  
399 Future experimentation using more intermediate L/V force ratio values, such as those seen in Figure 3c,  
400 will aid the understanding of the transition of pressure from the gauge to field side under an increasing  
401 lateral component of the resultant wheel load.

402 Having run several preliminary experiments in the laboratory, as well as developing a means to  
403 modify and protect the sensor for more accurate data collection, researchers at UIUC plan to instrument  
404 MBTSS on concrete crossties in the field. Field experimentation will allow analysis of actual loading  
405 conditions on the concrete rail seat surface with varying configurations of train loads, speeds, and track  
406 geometry. Another variable that we propose to investigate in field testing is the effect of TOR friction  
407 modification on the distribution of loads onto the rail seats of concrete crossties.

408 Field experimentation will also play a crucial role in guiding the future of laboratory  
409 experimentation. A good working relationship between field data and experimental data is expected as  
410 the pressure distribution data collection process is refined, and field conditions are better simulated in the  
411 laboratory.

412 In summary, the use of MBTSS appears to be a feasible, non-intrusive means to instrument  
413 concrete crossties to measure rail seat pressure distributions. Furthermore, results from this work will be  
414 leveraged, as the data collected from MBTSS in the laboratory and field will be used as an input for rail  
415 seat loads into finite element model (FEM) analysis of the concrete crosstie and fastening system  
416 currently being performed at UIUC.

417

#### 418 **ACKNOWLEDGEMENTS**

419 This research was funded by Amsted RPS / Amsted Rail Inc. and the United States Department of  
420 Transportation (US DOT) Federal Railroad Administration (FRA). The published material in this report  
421 represents the position of the authors and not necessarily that of DOT. J. Riley Edwards has been  
422 supported in part by grants to the UIUC Rail Transportation and Engineering Center (RailTEC) from CN,  
423 CSX, Hanson Professional Services, Norfolk Southern, and the George Krambles Transportation  
424 Scholarship Fund. For providing direction, advice, and resources the authors would like to thank Jose  
425 Mediavilla, Director of Engineering at Amsted RPS, Brent Wilson, Director of Research and  
426 Development at Amsted Rail, Mauricio Gutierrez from GIC Ingeniería y Construcción, Professor Jerry  
427 Rose and Graduate Research Assistant Jason Stith from the University of Kentucky, and Vince Carrara  
428 from Tekscan®, Inc. The authors would also like to thank Marc Killian, Tim Prunkard, and Don Marrow  
429 from the University of Illinois at Urbana-Champaign for their assistance in laboratory experimentation,  
430 and graduate students Ryan Kernes, Brandon Van Dyk, Brennan Caughron, Sam Sogin, and Amogh  
431 Shurpali for their peer review and editing and valuable input.

432

433

## 434 REFERENCES

- 435
- 436 1) International Heavy Haul Association. *Guidelines to Best Practices for Heavy Haul Railway*  
437 *Operations, Infrastructure Construction and Maintenance Issues*. D. & F. Scott Publishing, Inc.  
438 North Richland Hills, Texas, 2009, Ch. 1, 3, and 5, pp. 1-59, 3-67, 3-72, 5-2, and 5-6.
- 439 2) Zeman, J.C. Hydraulic Mechanisms of Concrete-Tie Rail Seat Deterioration, M.S. Thesis,  
440 University of Illinois at Urbana-Champaign, Urbana, Illinois, 2010, Ch. 1, 2, and 3.
- 441 3) Van Dyk et al 2012. *International Concrete Crosstie and Fastening System Survey – Final*  
442 *Results*, University of Illinois at Urbana-Champaign, Results Released June 2012.
- 443 4) Marquis, B.P, M. Muhlanger, D.Y. Jeong. Effect of Wheel/Rail Loads on Concrete Tie Stresses  
444 and Rail Rollover. *Proceedings of the ASME 2011 Rail Transportation Division Fall Technical*  
445 *Conference*, Minneapolis, Minnesota, September, 2011, pp. 1-3.
- 446 5) Rhodes, D. How Resilient Pads Protect Concrete Sleepers. *Railway Gazette International*,  
447 February, 1988, pp. 85.
- 448 6) American Railway Engineering and Maintenance-of-Way Association (AREMA). *AREMA*  
449 *Manual for Railway Engineering*, Landover, Maryland, Vol. 1, 2009, Ch. 30.
- 450 7) Lake, M., L. Ferreira, and M. Murray. Using Simulation to Evaluate Rail Sleeper Replacement  
451 Alternatives. In *Transportation Research Record: Journal of the Transportation Research Board*,  
452 No. 1785, Transportation Research Board of the National Academies, Washington, D.C., 2002, pp.  
453 4.
- 454 8) Rose, J.G., J.C. Stith. Pressure Measurements in Railroad Trackbeds at the Rail/Tie Interface  
455 using Tekscan Sensors. University of Kentucky, Lexington, Kentucky, pp. 1-20.
- 456 9) Kerchof, B., H. Wu. Causes of Rail Cant and Controlling Cant Through Wheel/Rail Interface  
457 Management. *Proceedings of the 2012 Annual AREMA Conference*, Chicago, Illinois, September,  
458 2012.
- 459 10) Costello, S.B., A.S. Premathilaka, and R.C.M. Dunn. Stochastic Rail Wear Model for Railroad  
460 Tracks. In *Transportation Research Record: Journal of the Transportation Research Board*, No.  
461 2289, Transportation Research board of the National Academies, Washington, D.C., 2012, pp. 4.
- 462 11) Gutierrez, M. J., J.R. Edwards, C.P.L. Barkan, B. Wilson, J. Mediavilla. Advancements in  
463 Fastening System Design for North American Concrete Crossties in Heavy Haul Service.  
464 *Proceedings of the 2010 Annual AREMA Conference*, Orlando, Florida, August, 2010, pp. 5.
- 465 12) *Handbook of Railway Vehicle Dynamics*, CRC Press, Taylor & Francis Group, Boca Raton,  
466 Florida, 2006, pp. 212.
- 467 13) Hay, W.W. *Railroad Engineering, 2nd ed.*, John Wiley & Sons, Inc., New York City, New York,  
468 1982, Ch. 23, pp. 471-473.
- 469 14) Giannakos, K., Loizos, A. Evaluation of actions on concrete sleepers as design loads – influence  
470 of fastenings. *International Journal of Pavement Engineering*, Vol. 11, Issue 3, 2010, pp. 209
- 471 15) Amtrak Engineering. Load Spectra of the Northeast Corridor. Presented at the 90<sup>th</sup> Annual  
472 Meeting of the Transportation Research Board, Washington, D.C., 2011.